Multidisciplinary Preclinical Investigations on Three Oxamniquine Analogues as Novel Treatment Options for Schistosomiasis

Valentin Buchter,[1,2,#] Yih Ching Ong,[3,#] François Mouvet,[4,#] Abdallah Ladaycia,[5] Elise Lepeltier,[5] Ursula Rothlisberger,[4,*] Jennifer Keiser,[1,2,*] and Gilles Gasser[3,*]

[1] Swiss Tropical and Public Health Institute, Socinstrasse 57, P.O. box, CH-4002 Basel, Switzerland.

[2] University of Basel, Petersplatz 1, P.O. Box, CH-4001 Basel, Switzerland.

[3] Chimie ParisTech, PSL University, CNRS, Institute of Chemistry for Life and Health Sciences, Laboratory of Inorganic Chemical Biology, F-75005 Paris, France.

[4] Laboratory of Computational Chemistry and Biochemistry, EPFL, 1015 Lausanne, Switzerland.

[5] MINT, UNIV Angers, INSERM 1066, CNRS 6021, Université Bretagne Loire, 4 rue Larrey, 49933 Angers Cedex 9, France.

[#] Contributed equally

* Corresponding authors: Email: ursula.roethlisberger@epfl.ch; WWW: https://www.epfl.ch/labs/lcbc/roethlisberger/; Tel. +41 21 693 03 21; jennifer.keiser@unibas.ch; WWW: https://www.swisstph.ch/en/about/mpi/helminth-drug-development/; Tel. +41 76 61 284 82 18; E-mail: gilles.gasser@chimeparistech.psl.eu; WWW: www.gassergroup.com; Tel: +33 1 85 78 41 51.

ORCID

Valentin Buchter: 0000-0002-1985-0676

Yih Ching Ong: 0000-0003-0411-1114

François Mouvet 0000-0002-0416-2598

Abdallay Ladaycia: 0000-0003-3931-0498

Elise Lepeltier: 0000-0002-7666-6453

Ursula Rothlisberger 0000-0002-1704-8591

Jennifer Keiser: 0000-0003-0290-3521

Gilles Gasser: 0000-0002-4244-5097

Keywords: Bioorganometallic Chemistry; Molecular Dynamics; Medicinal Inorganic Chemistry; Metabolic Stability; Oxamniquine; Schistosomiasis.

Abstract

Schistosomiasis is a disease of poverty affecting millions of people. Praziquantel (PZQ), with its strengths and weaknesses, is the only treatment available. We previously reported 3 lead compounds derived from oxamniquine (OXA), an old antischistosomal drug: ferrocene-containing (Fc-CH_2-OXA), ruthenocene-containing (Rc-CH_2-OXA) and benzene-containing (Ph-CH_2-OXA). These derivatives showed excellent *in vitro* activity against both *Schistosoma mansoni* and *S. haematobium* larvae and adult worms, and *in vivo* against *S. mansoni*. Encouraged by these promising results, we followed a guided drug discovery process and report in this investigation on metabolic stability studies, *in vivo* studies, computational simulations, and formulation studies. Molecular dynamics simulations supported the *in vitro* results on the target protein. Though all three compounds were poorly stable within an acidic environment, they were only slightly cleared in the *in vitro* liver model. This is likely the reason as to why the promising *in vitro* activity did not translate to *in vivo* activity. This limitation could not be saved by the formulation of lipid nanocapsules as an intent to improve the *in vivo* activity. Further studies should focus on increasing the compound's bioavailability, in order to reach an active concentration in the parasite's microenvironment.

Introduction

S. mansoni, S. haematobium and *S. japonicum* account for over 90% of the cases of schistosomiasis, an acute and chronic parasitic disease that affects over 200 million people worldwide[1-3] and faces more than 700 million people the risk of infection.[4] In children, schistosomiasis stunts physical growth and ability to learn, while in adults, the disease affects the ability to work, and can cause organ failure and ultimately death, a situation that causes an enormous socioeconomic burden for developing communities.[5] Praziquantel (PZQ), with its strengths and weaknesses, is the only drug being used for periodic mass drug administration to control the disease. Considering the threatening and real possibility of resistance[6] and that PZQ presents drawbacks, our efforts are oriented to identify and develop a new molecule with the potential to become an alternative therapeutic option in the treatment of this disease.

Oxamniquine (OXA, Figure 1) is an anthelmintic drug developed in the 1960s[7] that showed high activity and a very convenient drug profile in terms of safety and ease of administration. It became the cornerstone of the schistosomiasis eradication program in Brazil in the past and beginning of the 21st centuries but fell into disuse because of two main reasons: it was only active against adult *S. mansoni*[7-9] and resistance was clinically confirmed. The drug was therefore no longer commercialized after 2010 and replaced by PZQ.[7] OXA is a prodrug that needs the sulfotransferase of *S. mansoni* to be activated to an alkylating molecule that binds proteins and DNA, consequently killing the parasite.[10] Different enzyme orthologues are present in all S*chistosoma* species, however only the active site of the sulfotransferase of *S. mansoni* can activate OXA.[11] The mechanism of resistance and lack of activity in the remaining species has been well studied. Resistance is based in one or more punctual mutations in the enzyme's active site that prevent the molecule to be sulfonated.[12] Taking into account that there is a 70% homology between the amino acid sequences of the sulfotransferases of *S. mansoni* and *S. haematobium*,[11] we derivatized OXA

based on the hypothesis that modification of OXA could overcome the species and stage specificity. [13]

Previous studies by Jaouen and co-workers on the anticancer drug candidate ferrocifen[14-16] and Brocard, Biot and co-workers on the anti-malarial drug candidate ferroquine showed that the ferrocenyl analogues of tamoxifen and chloroquine, respectively have improved bioactivity compared to the original organic drug compounds.[17, 18] This was due to several factors: the ferrocenyl component acted as a producer of reactive oxygen species (ROS), increased the lipophilic character of the molecule and provided a mechanism of action different to that of the original drug.[19-21] With this concept in mind, we developed several metal-containing derivatives of OXA, which were studied *in vitro* and *in vivo* against *Schistosoma spp.* [22-24] Among others, we demonstrated that the three derivatives of OXA, namely a ferrocene- (Fc-CH_2-OXA), ruthenocene- (Rc-CH_2-OXA) and benzene-containing (Ph-CH_2-OXA) derivative (Figure 1), showed promising *in vitro* results, where all three OXA derivatives caused death of *S. mansoni* and *S. haematobium* larval and adult worms[24] and worm burden reductions of 76 to 93% against adult *S. mansoni in vivo*.[22]

Encouraged by our promising preliminary results, we decided to go further in the development and to fully characterize these three OXA analogues. *In vitro* studies were conducted against *S. mansoni* juvenile worms, and *S. japonicum* and *S. haematobium* adult worms. *In vivo* studies were carried out against adult *S. haematobium* and juvenile *S. mansoni* including studies with Ph-CH_2-OXA encapsulated in Lipid NanoCapsules (LNC). Our work was complemented by computational models and molecular dynamics simulations as well as microsomal stability and albumin binding studies.

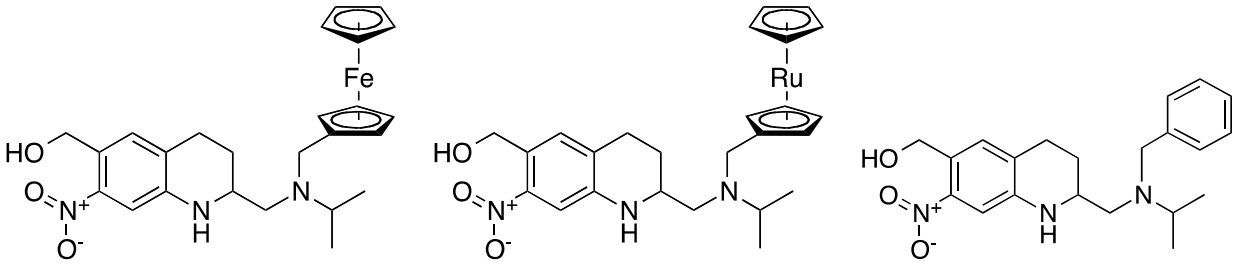

Fc-CH_2-OXA **Rc-CH_2-OXA** **Ph-CH_2-OXA**

Figure 1. Structures of the compounds investigated in this study.

EXPERIMENTAL SECTION

Materials and methods

All chemicals were either commercially available or were prepared following standard literature procedures. Solvents were used as received or distilled using standard procedures. All preparations were carried out using standard Schlenk techniques.

^{1}H and ^{13}C NMR spectra were recorded in deuterated solvents on Bruker 400 or 500 MHz spectrometer at room temperature. The chemical shifts, δ, are reported in ppm (parts per million). The residual solvent peaks have been used as internal references. The abbreviations for the peak multiplicities are as follows: s (singlet), d (doublet), t (triplet), m (multiplet). ESI mass spectrometry was performed using a LTQ-Orbitrap XL from Thermo Scientific. Elemental analysis was performed at Science Centre, London Metropolitan University using Thermo Fisher (Carlo Erba) Flash 2000 Elemental Analyser, configured for % CHN.

OXA-Derivatives preparation

The OXA derivatives were prepared starting from the parent compound oxamniquine (Pfizer) as described previously.[22] The analytical data matched that previously reported.[22]

Animals and parasites

All animal experiments were conducted at the Swiss Tropical and Public Health Institute (Swiss TPH) and authorized by the animal welfare office Kanton Basel Stadt, Switzerland (Authorization no. 2070).

NMRI female mice were purchased from Charles River (Sulzfeld, Germany) at the age of three weeks and were left without intervention for one week of acclimatization. Mice were infected with a subcutaneous infection of around 100 cercariae in the back of the neck, following the procedure described by Lombardo *et al*. [25]

For the *S. haematobium* chronic infection, one-month old LVG hamsters (Charles River, NY) were provided by the National Institutes of Health (NIH)–National Institute of Allergy and Infectious Diseases (NIAID) Schistosomiasis Resource Center (SRC) for distribution by the Biomedical Research Institute in Rockville, USA, which were pre-infected with 350 *S. haematobium* cercariae. The animals were kept in the animal facility with humidity and light control (50 % - 12/12) for three months.

Swiss Webster mice infected with *S. japonicum* (Philippine strain) were also obtained from NIH NIAID SRC for our *in vitro* studies.

***In vitro* studies**

Adult *S. mansoni, S. haematobium* and *S. japonicum* worms were collected by dissection from the mesenteric veins. Until use (within 24 h after dissection) and during the experiments, the worms were kept in the incubator by 37°C and 5% CO_2 and the culture medium consisted of RPMI 1640 (Gibco - Thermofisher, Waltham, MA USA) supplemented with 1% penicillin/streptomycin (BioConcept, Allschwil, Switzerland) and 5% Fetal Calf Serum (FCS) (BioConcept). The control groups consisted of culture medium spiked with dimethyl sulfoxide (DMSO) at a concentration of 1% or 0.5%, equivalent to the content of DMSO present in the wells of worms treated with the highest drug concentration for that assay. The concentrations evaluated were 100, 50, 25, 12.5

and 6.25 µM. The studies on *S. mansoni* and *S. japonicum* were performed as duplicates and repeated once, while the studies on *S. haematobium* were performed in duplicates. Every study condition included at least three worms.

We further evaluated the effect of the addition of albumin (AlbuMAX II, Gibco) to the culture medium to investigate if the activity of the derivatives was different. For this we set the same assay design as described before and added 45 g/l albumin to the culture medium, corresponding to the content of albumin within the range of human plasma.[26] We performed the study with medium containing albumin on adult *S. mansoni* (duplicate and repeated once), and on adult *S. haematobium* (on duplicate). To assign a score to the viability, we used a previously described method[27] scoring motility, viability, and morphological alterations using a bright field inverted microscope (Carl Zeiss Oberkochen, Germany, magnification ×4 and ×10).

***S. mansoni juvenile* worms for *in vitro* studies**

28 days after infection, mice were euthanized and juvenile worms were obtained by blood perfusion. The perfusion solution consisted of 8.5 g/L NaCl, 7.5 g/L Na-citrate in distilled water. Parasites were in different stages of development, as reported somewhere else.[28] All juvenile worms were kept in culture medium as described before for adult *S. mansoni* until use within 24 h. To test the activity of the derivatives against the juvenile stages, we incubated the worms with a 100 µM concentration of each of the derivatives in duplicates and at least two worms per well. Duplicates of 100 µM OXA and 1 % DMSO served as control conditions.

Calculation of IC_{50} values

CompuSyn 1.0 (ComboSyn Inc, 2007) was used to calculate the IC_{50} values of each of the derivatives after an incubation period of 72 h. The following equation was used to normalize the scores of the treated worms to the controls:

$$\text{Effect} = 1 - \frac{\text{average score treatment}}{\text{average score control}}$$

Drug suspension for oral administration

The derivatives were administered to the animals in form of an oral suspension. The compounds were first dissolved in DMSO (Sigma-Aldrich, Buchs, Switzerland) corresponding to 10% of the total volume, and then a mixture of Tween 80 and ethanol in a proportion of 70:30 was added, also corresponding to 10% of the final volume. The remaining 80% of the volume consisted of distilled water, which was added under stirring by small aliquots.

In vivo* activity on juvenile *S. mansoni

21 days after infection, mice were treated orally with each of the derivatives and the nanocapsules loaded with Ph-CH_2-OXA at a concentration of 200 mg/kg. Four weeks after treatment (seven weeks after infection), when the worms reached the adult stage of development, the mice were euthanized with CO_2, dissected and the remaining alive worms were picked out from the mesenteric veins and liver, sexed and counted.

In vivo* activity on adult *S. haematobium

The hamsters harboring an adult infection were treated with a dose of 200 mg/kg of the compounds. Three weeks after treatment, the hamsters were euthanized with CO_2, dissected and the worms were picked out from the mesenteric veins and liver, sexed and counted.

Computational studies

Classical molecular dynamics simulations were performed of the target proteins, i.e. the sulfotransferase of *S. mansoni* (SmSULT) and of *S. haematobium* (ShSULT), in complex with **OXA**, **Fc-CH_2-OXA** and **Ph-CH_2-OXA**. Since the two enantiomers of **OXA** show different activities against schistosomes,[29, 30] we performed separate simulations for both enantiomeric forms of all molecules.

To develop force field parameters for the drugs, the geometry of all compounds was optimized in the gas phase with the Gaussian 16 software package,[31] using DFT with B3LYP functional and a 6-31+G* basis set for non-metallic atoms and LANL2DZ pseudopotential for the iron atom. The initial geometries were taken from crystallized *S*-OXA complexed to SmSULT (PDB: 4MUB[11]). Hess *et al.* crystallized in 2017 the *R*-enantiomer of Fc-CO-OXA[22] and we used this structure as a starting point for all *R*-isomers and for comparison, since Fc-CO-OXA showed weak activity against *S. mansoni in vitro* in that previous experimental work . The electrostatic potential was computed with the same functional and basis set in order to estimate the effective atomic point charges through RESP fitting.[32]

Classical molecular dynamics simulations were performed using Amber16.[33] The protein was modelled using the FF14SB force field and the Generalized Amber Force Field 2 (*gaff2*) was used as a base for the ligands. The ferrocenyl group was modelled using the force field published by Doman *et al.*[34] To estimate the missing dihedral parameters between the ferrocenyl group and the rest of the molecule, we scanned the angles of interest and performed DFT single point energy calculations for all angles, using the same functional, basis set and pseudopotential as for the geometry optimization. We then used the software *paramfit* from AmberTools16[33] to estimate the parameters. To prevent clashes between nuclei during the rotation, we performed these computations on subsystems containing solely atoms that are relevant for these parameters (e.g. Fc-CH_2-NH_2, Fc-CH_2-N-$(CH_3)_2$, Fc-CO-NH_2 and Fc-CO-N-$(CH_3)_2$). All parameters determined in this way accurately reproduce the corresponding *ab initio* energy profiles (Figure S5).

The crystallographic structures of SmSULT and ShSULT with OXA and the cofactor 3'-phosphoadenosine-5'-phosphate (PAP) served as a starting point for our simulations (PDB: 4MUB and 5TIY,[30] respectively). OXA was replaced by its derivatives through alignment of their shared atomic groups. 3'-phosphoadenosine-5'-phosphosulfate (PAPS), the active version of PAP, was

inserted in the same way by minimizing the distance between shared PAP atoms. Missing loops of the protein were added using the ModLoop web server.[35] Using *tleap*, the resulting system was put in a 84x84x84 $Å^3$ periodic box filled with explicit TIP3P water molecules. Finally, the total charge was neutralized by adding Na^+ counter-ions. The resulting systems consisted of about 50'000 atoms.

Classical trajectories were computed using Amber's CUDA version of the PMEMD program. After minimization, the SHAKE algorithm[36] was used to constrain covalent bonds involving hydrogen atoms and the system was heated to body temperature (T = 310 K) in two steps using a Langevin thermostat. First, the water molecules were heated to the target temperature while restraining the positions of the ligand and protein during 50 ps with a time step of 1 fs. Then, the restraints were released and the whole system was thermalized in the NPT ensemble for 400 ps, with a time step of 1 fs and a pressure relaxation time of 3 ps. We then performed NPT simulations for 40 ns with a time step of 2 fs to reach an equilibrium state of the system. We finally performed 80 ns NPT production runs that were used for analysis.

The binding free energy of the ligands inside the protein was estimated based on the MD trajectories using two methods available in Amber16: Generalized Born Surface Area (MM/GBSA) and Poisson Boltzmann Surface Area (MM/PBSA).[37]

pH and metabolic stability studies

The stability of the three OXA derivatives was studied by *in vitro* co-incubation with acidic environment. To 200 µL of HPLC grade MeCN in a 1.5 mL Eppendorf, 2 µL of 37 % HCl were added to form a final 0.1 M HCl solution. 10 µL test compound (5 mM in HPLC MeCN) were then added to this acidic solution. For the non-acidic control samples, 10 µL test compound (5 mM in HPLC MeCN) were added to 200 µL of HPLC grade MeCN. The compounds were then incubated for 24 h at 37 °C and assessed at t = 0 h and t = 24 h.

Analytical HPLC measurement was performed using a 1260 Infinity HPLC System (Agilent Technology) comprising: 2 x Agilent G1361 1260 Prep Pump system with Agilent G7115A 1260 DAD WR Detector equipped with an Agilent Pursuit XRs 5C18 (100 Å, C18 5 µm 250 x 4.6 mm) Column. The solvents were acetonitrile (HPLC grade) and purified water (Pacific TII) with flow rate 1 mL/min. Detection was performed at 215 nm, 250 nm, 350 nm, 450 nm, 550 nm and 650 nm with a slit of 4 nm. The flow rate was 1 mL/min and the max pressure was set 200 bar. Run parameters were as follows: 0 min 85 % acetonitrile (MeCN) 15 % H_2O; 3 mins 85 % MeCN 15 % H_2O; 7 min 100 % MeCN ; 9 min 100 % MeCN , 11 min 85 % MeCN 15 % H_2O.

The metabolic stability of the three OXA derivatives was studied by *in vitro* co-incubation with human liver microsomes. All three compounds were incubated in the presence of NADPH at 37 °C. The protocol was adapted from previous studies:[38, 39] 10 µL of 20 mg/mL microsomes (GIBCO, 50 pooled), 463 µL of PBS (GIBCO, 1x PBS) and 2 µL of 40 mM NADPH (Sigma) were added to 1.5 mL Eppendorf tubes and incubated at 37 °C for 10 min to prime the microsomes. Following this, 10 µL of 50 mM test compound and an additional 15 µL of NADPH were added (1 mM final concentration of test compound in 500 µL total volume). The samples were incubated at 37 °C, and quenched at the desired time points of 1, 4 and 24 h by adding 2 mL of dichloromethane (DCM) or any other organic solvent. 2.5 µL of 5 mM caffeine (TCI Chemicals) in HPLC MeCN as internal standard were added during the quenching process. The mixture was shaken for 10 min to ensure complete extraction. The DCM layer was carefully removed and then evaporated to provide residues that were analyzed by LC-MS (HPLC Waters 2525/Mass Spectrometry Waters ZQ 2000) using a pure acetonitrile-water system with the same column as above. The residues were dissolved in 100 µL HPLC grade acetonitrile. 20 µL from each MeCN residue sample was injected manually using the following run parameters: 3 min 5 % MeCN 95 % H_2O; 13 min 40 % MeCN 60 % H_2O; 14 min 100 %

MeCN 0 % H_2O; 20 min 100 % MeCN 0 % H_2O; 23 min 5 % MeCN 95 % H_2O. UV spectra were analyzed and compared at different time points.

By comparing the differences in respective *m/z* values in MS spectra, *m/z* values for the parent compound and OXA could be identified. Semi-quantitative analysis of the ratio of parent compound and different metabolites present in the mixture after incubation with human liver microsomes was achieved by comparing the areas under the respective peaks of different compounds visible in the UV traces of the LC analysis at 245 nm. To determine the *in vitro* half-life ($t_{1/2}$), the following process was derived from Tan *et al.*[40]

The peak areas of the compounds at different time points are expressed first as a percentage of the internal standard, caffeine.

$$\text{Ratio at timepoint} = \frac{\text{Area under curve of compound}}{\text{Area under curve of internal standard}}$$

Following this, normalized ratios were calculated using the ratio of peak area of the test compounds to caffeine at t = 0 h. Normalised ratios were calculated at each assessed timepoint of t = 1 h, 4 h and 24 h.

$$\text{Normalised ratio} = \frac{\text{Ratio at timepoint} \neq 0}{\text{Ratio at timepoint} = 0}$$

The normalized ratio values are then plotted against incubation time. The $t_{1/2}$ values calculated via analyses methods in GraphPad Prism 8 (nonlinear regression, exponential one phase decay). The degradation rate constant, k was then calculated using the $t_{1/2}$ values (converted from hours to minutes).

The predicted *in vitro* intrinsic clearance values (expressed as µL/min/mg protein) were then calculated as a ratio of the degradation rate constant *k* (expressed as min^{-1}) and the microsomal protein concentration (mg/µL).

$$\textit{in vitro}\ \text{intrinsic clearance values}\ CL_{int} = \frac{k}{\text{microsomal protein content (0.4 mg/mL protein)}}$$

Ph-CH_2-OXA loaded lipid nanocapsules

Lipid nanocapsules (LNC) were formulated by the phase inversion phase method.[41] Briefly, to prepare blank LNC, Labrafac® (Gattefossé SAS, France, 20.6 % w/w), Lipoid® S 100 (Ludwigshafen, Germany 1.5 % w/w), Kolliphor HS 15 (Florham Park, USA 17 % w/w), NaCl (Sigma-Aldrich, USA 1.3 % w/w) and water (59.6 % w/w) were mixed and homogenized under magnetic stirring at 80 °C. Three cycles of progressive heating and cooling between 90 °C and 50 °C were then performed. During the last cooling cycle, the mixture was diluted by adding 2 °C purified water (28.7 % v/v) in order to induce an irreversible shock and formulate LNC. In order to encapsulate Ph-CH_2-OXA inside the LNC, some slight changes to this protocol have been applied. The Ph-CH_2-OXA (4.35 % w/w) was mixed with Labrafac®, Lipoid® S 100 and ethanol (Fisher, USA) to help solubilization of the molecule in the lipid phase. This mixture was put under agitation at 50 °C until total solubilization of the Ph-CH_2-OXA. The ethanol was then evaporated under argon. Once the ethanol evaporated, Kolliphor HS 15, NaCl and water were added and three heating and cooling cycles were performed as prescribed for formulating blank LNC. During the last cooling cycle, the mixture was diluted by adding 2 °C purified water. Empty LNC and Ph-CH_2-OXA loaded LNC were characterized using Dynamic Light Scattering (DLS) to determine their size, polydispersity index (pdi) and zeta potential.

Results and Discussion

In vitro studies

Fc-CH_2-OXA, Rc-CH_2-OXA and Ph-CH_2-OXA previously demonstrated promising activity as drug candidates *in vitro* against adult *S. mansoni* and S. *haematobium* and first stage of the larval development (NTS: newly transformed schistosomula) and *in vivo* in adult *S. mansoni* infected mice.[22, 24] In order to test the full potential of our compounds, we first elucidated the *in vitro* activity of the OXA derivatives against 28-day-old juvenile *S. mansoni* worms since one of the important drawbacks of PZQ is its missing activity against this developmental stage. All three compounds killed all the worms within 24 h of incubation at a concentration of 100 µM (Table 1). Against juvenile *S. mansoni*, Rc-CH_2-OXA had the lowest IC_{50} (3.7 µM) while Ph-CH_2-OXA was the drug with the highest IC_{50} value (26.7 µM), therefore the one with the lowest activity. Interestingly, in the case of Ph-CH_2-OXA, the effect of the molecules on the juveniles was faster than against the adults: while on adult *S. mansoni,* Ph-CH_2-OXA needed 72 h to exert its maximal activity; against juvenile stages, we observed a total effect within 24 h of incubation at a dose of 100 µM. For comparison, by the same incubation time, juvenile *S. mansoni* incubated with 100 µM OXA and the control group showed no difference in the viability, confirming previous studies of OXA being only slightly active *in vitro* and against juvenile stages of the parasite.[9, 24] Only by 72 h of incubation, where the derivatives had long exerted their activity, we found a 38% reduction of the viability of OXA respect to the control worms.

Against *S. japonicum* adult worms, we observed the same behavior: while OXA was not active even by 100 µM after 3 days (Table 1), our derivatives showed considerable activity. Of the three derivatives tested, Fc-CH_2-OXA proved to be the most active of all three derivatives, killing all the parasites within 24 h at a concentration of 100 µM and having the lowest IC_{50} value (22.6 µM). On

S. haematobium instead, the most active compound was Rc-CH_2-OXA, also killing all parasites by a concentration of 100 µM and revealing the lowest IC_{50} value (15.5 µM).

Moreover, we incubated adult *S. mansoni* in medium containing albumin and compared the activity determined to our standard assay. A lower activity of the three drugs was observed in the enriched medium, with Fc-CH_2-OXA showing the least loss of activity of the three derivatives (Table 1). The albumin binding experiment was also performed for adult *S. haematobium.* Also in this case, the three compounds showed a reduction of the activity. These results are comparable with those obtained by Pasche *et al,*[42] who also identified a significant decrease in drug activity incubating antischistosomal drug candidates *in vitro* in the presence of albumin. Also, PZQ presents a high percentage (around 80%) of drug bound to protein[43] and this might be one of the reasons for the high doses needed to reach a significant effect. Protein binding is a major issue in drug development, since only the free fraction of the drug is able to interact with the target.[44]

Table 1. *In vitro* activity of Fc-CH_2-OXA, Rc-CH_2-OXA and Ph-CH_2-OXA versus OXA against *S. mansoni*, *S. haematobium* and *S. japonicum*.

	S. mansoni				***S. haematobium***		***S. japonicum***
Compound	**IC_{50} adults 72 h (µM)**	**IC_{50} adults in medium 45 g/L albumin. 72 h (µM)**	**Onset of action on juveniles 100 µM (h)**	**IC_{50} 28 day juveniles 72 h (µM)**	**IC_{50} adults 72 h (µM)**	**IC_{50} adults in medium with albumin. 72 h (µM)**	**IC_{50} adults 72 h (µM)**
Fc-CH_2-OXA	9.0	28.1	< 24	5.8	52.3	55.7	22.7
Rc-CH_2-OXA	6.0	NC	< 24	3.8	15.5	25	30.9
Ph-CH_2-OXA	13.5	90.7	< 24	26.7	32.6	70.6	39.8
OXA	>100	>100	72	> 100	>100 *	ND	>100

* Hess et al.[22] , NC: no correlation, ND: not done.

Studies on juvenile *S. mansoni* in the mouse model

In terms of activity against juvenile parasites *in vivo*, we identified a lower activity of all three compounds in respect to the results on adult parasites.[22] Worm burden reductions ranged from 39 to 47% (Table 2). Some worms remained alive despite being moderately affected by the drug, as shown by their shift to the liver due to the loss of vein attachment.

Table 2: Reduction of the juvenile worm burden in *S. mansoni* infected mice after treatment with 200 mg/kg of the OXA derivatives and after treatment with the nano encapsulated Ph-CH_2-OXA.

Compound	No. of mice	Worm burden (SD)		WBR % pure drug		WBR % nanocapsule	
		Females	Total	Females	Total	Females	Total
Control	8	6.5 (1.6)	12.3 (2.5)	-	-		
Fc - OXA	4	3.8 (0.96)	7.5 (2.65)	41.5	38.8	ND	ND
Rc - OXA	4	3 (2.45)	6.5 (4.43)	53.8	46.9	ND	ND
Bn - OXA	4	4.3 (0.5)	7.5 (0.58)	33.8	38.8	0	0

ND: Not done; WBR: worm burden reduction

In vivo* studies on adult *S. haematobium

Table 3 shows the worm burden reduction of the three compounds against *S. haematobium*: none of the compounds affected *S. haematobium in vivo,* contradicting the findings observed *in vitro*.

Table 3: Reduction of the worm burden of *S. haematobium* infected hamsters after treatment with 200 mg/kg of the OXA derivatives.

Compound	No. of mice	Worm burden (SD)		WBR %
		Females	Total	
Control	4	18.5 (8.3)	40 (13.6)	-
Fc-CH_2-OXA	4	25.8 (7.5)	54 (16.2)	0
Rc-CH_2-OXA	3	55 (16.1)	108 (28.9)	0
Ph-CH_2-OXA	4	19 (3.7)	51 (18.9)	0

Computational studies

In order to understand the interaction between OXA analogues and the sulfotransferase proteins from *S. mansoni* (SmSULT) and *S. haematobium* (ShSULT), we performed classical molecular dynamics simulations of OXA, Fc-CH_2-OXA, and Ph-CH_2-OXA to determine their binding poses within the active site of the two sulfotransferases at body temperature. We did not consider Rc-CH_2-OXA explicitly since both from a geometrical and electrostatic point of view, we expect the ferrocenyl and ruthenocenyl compounds to yield similar results at this simplified level of theory.

The free energy difference between bound and unbound states of a receptor-ligand complex is a direct measure of the binding affinity. To estimate this quantity from our trajectories, we used the MM/PBSA (Table 4) and MM/GBSA methods (Table S1). All binding free energies are negative, meaning that the bound state is energetically favorable for all compounds. No systematic difference can be noted between the two proteins and all modified OXA compounds show a higher binding affinity than OXA itself. This is probably due to their larger size, forcing a tighter fit inside the protein and increasing the number of interactions with the binding pocket. Consequently, all analogues are strongly bound to their target proteins.

Table 4. Estimated binding free energies computed by the MM/PBSA method (kcal/mol).

	S. mansoni		***S. haematobium***	
	R	***S***	***R***	***S***
Fc-CH_2-OXA	-39.3	-41.9	-36.3	-39.9
Fc-CO-OXA	-36.3	-29.9	-26.4	-32.0
Ph-CH_2-OXA	-30.3	-35.0	-36.6	-18.3
OXA	-12.5	-8.0	-17.1	-22.8

Since the drugs are supposed to react with PAPS within the target protein, the distance between the closest oxygen of the sulfate group of PAPS and the hydrogen in the hydroxyl group of each drug was measured every 40 ps. These distances are represented as histograms in Figure 2 and their average is shown in Table 4. The near-attack configurations (NAC), i.e., the ones with shorter distances between the reactive groups are more likely to result in the activation of the compounds.

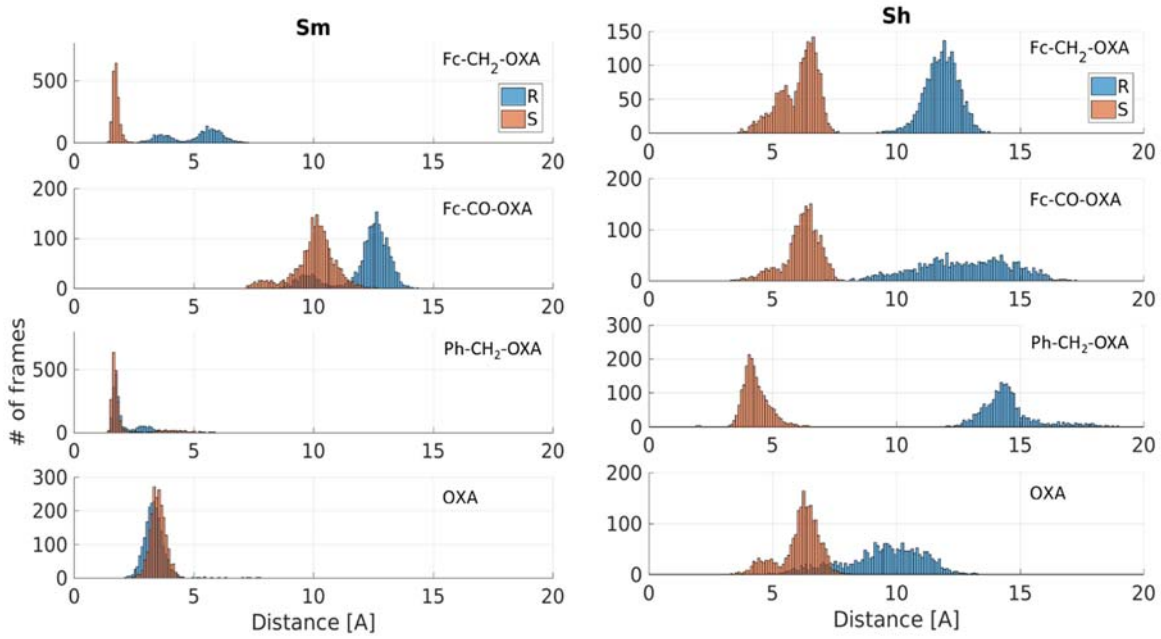

Figure 2. Distance between the closest oxygen of PAPS and the hydroxyl group of the analogues. *R*-enantiomers in blue and *S*-enantiomers in orange.

Table 5. Average O-H distance with standard deviation (Å)

	S. mansoni		***S. haematobium***	
	R	***S***	***R***	***S***
Fc-CH_2-OXA	5.1 ± 1.1	1.8 ± 0.1	11.8 ± 0.7	6.1 ± 0.8
Fc-CO-OXA	12.2 ± 1.2	10.0 ± 0.9	12.8 ± 1.9	6.2 ± 0.7
Ph-CH_2-OXA	2.2 ± 0.7	2.0 ± 0.7	14.5 ± 1.1	4.3 ± 0.5
OXA	3.3 ± 0.4	3.5 ± 0.3	9.5 ± 1.6	6.1 ± 0.8

For OXA in SmSULT, the sulfate-hydroxyl distance is short and stable for both enantiomers, with an average slightly above 3 Å. The relative orientation of the reactive groups is fixed through their mutual interaction with ASN230, thus promoting the interaction (Figure S2). The chain of residues 19 to 23 also binds to PAPS and OXA at different places, stabilizing the configuration. For OXA, the difference between *R*- and *S*-enantiomers is very small, which is consistent with previous experimental works that already reported that both enantiomers bind in a similar fashion and that the activity difference originates from their binding kinetics.[29]

Both enantiomers of Ph-CH_2-OXA and Fc-CH_2-OXA show a very strong interaction with PAPS within SmSULT. Residues 18 to 21 bind both ligands in several places, highly stabilizing their binding (Figures S4 and S6). Moreover, the residue ASN230 also binds to PAPS and to the chain of residues 18-21, further increasing the stability. This may explain the high activity of these compounds *in vitro*. On the other hand, the *R*-enantiomer of Fc-CH_2-OXA seems to drift slowly away from PAPS and a proper equilibrium is never reached within our simulation time. The distance increases over time, which suggests that the final configuration will not be active. Strikingly, Ph-CH_2-OXA does not seem to be impacted by the enantiomer selectivity observed for all other derivatives.

Fc-CH_2-OXA, that was the most active against *S. mansoni* according to the *in vitro* experimental studies, shows short average distance to PAPS. In *S. haematobium* instead, the shortest distance to PAPS is held by the *S*-enantiomer of Ph-CH_2-OXA, which also shows a lower IC_{50} against this species when compared to Fc-CH_2-OXA. Furthermore, our simulations of Fc-CO-OXA in SmSULT show NAC distributions where the reactants are about 3 times more distant than in OXA, with averages above 10 Å. These configurations are very unlikely to activate the drug, which is again consistent with experimental results.

In practice, OXA is not active on *S. haematobium*. In simulations where OXA is docked into ShSULT, we observe that the distance between the reactive groups is much larger than in SmSULT, by more than 6 Å on average. Furthermore, we observe a large difference between enantiomers, where the *R*-enantiomer shows a broad distribution of NAC distances with an average of 9.5 Å. This strong enantiomer dependence is present for all compounds and is more pronounced than in SmSULT with all *R*-enantiomers adopting less reactive configurations. The residue ASP80 seems to have a negative impact, forming a stable bond with the drug's hydroxyl group (Figures S3, S5, S7). This bond is far from PAPS, leading to unreactive geometries shown by a widening of the distance

distributions between the compounds and PAPS. This residue is conserved in SmSULT, but stays at larger distances (more than 4.5 Å from the hydroxyl group of all considered compounds).

In ShSULT, the *S*-enantiomer of Ph-CH_2-OXA shows the most promising results. Our *in vitro* experiments showed that this compound was active against *S. haematobium* and our structures show significant improvements over OXA. The distances between reactant groups are significantly smaller, at about 4.3 Å on average and only slightly larger than for OXA in SmSULT, indicating that the compound could be activated. We also noticed that the difference between enantiomers is much larger in ShSULT than in SmSULT, suggesting that using enantiopure samples of the drug instead of racemic mixtures may significantly improve the drug's efficacy against *S. haematobium*.

Stability of OXA Analogues in Acidic Environments and in the Presence of Microsomes

We further investigated if the reduction of *in vivo* activity could be explained by physiological stability issues. We therefore evaluated two different conditions: an acidic environment and the co-incubation in the presence of liver microsomes, to simulate the environments within the stomach and the liver, respectively.

Under acidic conditions, all candidates showed little stability after 24 h exposure to 1 M HCl. As only a qualitative answer was needed, simple HPLC methods with a short run time were used to visually check the elution of the fragments before and after exposure to 1 M HCl (Figure S8). Compared to Fc-CH_2-OXA, which elutes at 1.9 min, the main species in the presence of acid, elutes at 2.7 min, with other minor species eluting at 1.8 and 2.5 min. Rc-CH_2-OXA elutes at 2.0 min, while the main species in presence of acid elutes at 2.7 min, and other minor peaks at 1.7 min. Ph-CH_2-OXA elutes at 1.9 min, while the main species in the presence of acid elutes at 2.8 min, followed by minor peaks eluted at 2.6 min. Since all compounds after 24 h incubation with 1 M HCl produce

completely different elution peaks after incubation, all three compounds have little stability in acidic media.

We conducted the metabolic stability assays using commercially available human liver microsomes, which are specific for Phase I processes catalyzed by cytochrome P450 (CYP) monooxygenases and flavin containing monooxygenases (FMO). We selected human instead of animal based microsomes as human clinical outcomes can be assessed. The incubation time is extremely long compared to usual incubation times because these compounds have shown high stability beyond 1 h.

The metabolic stability results are summarized in Table 6. The stability of the compounds decreased exponentially with > 40 % compound remaining after 24 h, with similar half-life values ranging from 2.2 – 3.8 h. The intrinsic clearance of the compounds was low and intermediate ranging from 7.5 to 13.3 μL/min/mg.[45]

Table 6. Metabolic stability in human microsomes

Compound	$t_{1/2}$ (h)	k (min^{-1})	CL_{int} (μL min^{-1} mg^{-1})
Fc-CH_2-OXA	3.8	0.0030	7.5
Rc-CH_2-OXA	2.2	0.0053	13.3
Ph-CH_2-OXA	2.4	0.0048	12.0
OXA	3.1	0.0037	9.3

The elution peaks showed in Figure S11 evidence that only the Ph-CH_2-OXA derivative remained unchanged in a tolerable amount after 24 h of metabolic stability evaluation.

From the values of intrinsic clearance in Table 6, according to McNaney *et al.*, Fc-CH_2-OXA could be categorized as “low” clearance, while Rc-CH_2-OXA, Ph-CH_2-OXA and OXA would be categorized as “intermediate”.[46, 47] It is also shown that the Ph-CH_2-OXA derivative has the second highest CL_{int} value while showing little change in the mass spectra.

The elution peaks showed in Figure S9, S10 and S11 for Fc-CH_2-OXA, Rc-CH_2-OXA and Ph-CH_2-OXA respectively are evidence that only the Ph-CH_2-OXA derivative remained unchanged in an acceptable 56 % after 24 h of incubation in the presence of microsomes (Figure S11). The spectra shows visually no difference before and after microsomal exposure, which indicates that the Ph-CH_2-OXA derivative was resistant to microsomal oxidation, hydroxylation and reduction compared to its metallocenyl analogues, Fc-CH_2-OXA and Rc-CH_2-OXA. Based on these results, it was decided to select Ph-CH_2-OXA for lipid nanoencapsulation studies. This would allow us to determine if nanoencapsulation reveals a better delivery of the compound to its parasitic targets.

Lipid Nanocapsules loaded with Ph-CH_2-OXA

In order to enhance the bioavailability, Ph-CH_2-OXA was loaded into lipid nanocapsules as both computational and metabolic stability results showed this candidate to be favourable for formulation improvement. Lipid nanocapsules are the vector of choice to encapsulate lipophilic molecules[48] as they have been intensively used for *in vivo* administration of ferrocifens. [49-52]

Ph-CH_2-OXA was encapsulated at a concentration of 32.35 mg per mL of LNC, representing a drug loading of 4.35 % w/w. The physico-chemical parameters (characterized by Dynamic Light Scattering), of blank LNC and Ph-CH_2-OXA loaded LNC were the same: diameters of approximately 50 nm, a pdi value below 0.2, which demonstrates a monodispersed population of nanoobjects, and a zeta potential close to neutrality as shown in Table 7.

Table 7. Physico-chemical parameters characterized by DLS of empty LNC (blank) and Ph-CH_2-OXA loaded LNC

	Diameter (nm)	**pdi**	**Zeta potential (mV)**
Blank LNC	57.4 ± 0.9	0.07 ± 0.02	-3.9 ± 0.7
Ph-CH_2-OXA LNC	53.0 ± 0.5	0.04 ± 0.02	-3.1 ± 0.1

The *in vivo* activity of the drug loaded nanocapsules was evaluated in mice harboring a 21-day *S. mansoni* infection but this improvement in formulation was not translated into a raise of the activity, as observed in Table 2. The low activity could be the result of a slow or even an absence of drug release, and/or a limited pathogen LNC internalization.

Conclusions

In this study, we followed up on three OXA analogues that had shown promising antischistosomal activity. The computational models forecast that the ferrocene- and benzene-containing analogues sample far more near attack configurations with the target sulfotransferase than the parent compound (OXA) for *S. mansoni.* On the contrary, in *S. haematobium*, only the *S*-enantiomer of Ph-CH_2-OXA shows the most significant improvement over OXA and could be active against this species. These findings correlated exactly with the *in vitro* results. When considering the *in vivo* studies instead, we evidenced a lack of activity for all three derivatives against juvenile *S. mansoni* and adult *S. haematobium.* We found that all three compounds were poorly stable within an acidic environment but were only slightly cleared in the *in vitro* liver model. This is likely the reason as to why the promising *in vitro* results did not translate to *in vivo* activity. We further evaluated if the lipid nanoencapsulation of the lead compound (Ph-CH_2-OXA) could overcome this limitation, but unfortunately the formulated compound was also inactive. Since the bioavailability and not the activity on the target seems to be the main limitation of these molecules, further steps in this strategy should include a study on gastro resistant ways of drug administration, to find out if the improved bioavailability can overcome the loss of *in vivo* activity.

Conflict of interest

There are no conflicts to declare.

Acknowledgements

This work was financially supported by the Swiss National Science Foundation (Grant Sinergia CRSII5_173718) and has received support under the program «Investissements d'Avenir» launched by the French Government and implemented by the ANR with the reference ANR-10-IDEX-0001-02 PSL (G.G.). We are grateful for the loan of analytical instruments by Agilent Technologies and CEA Saclay to Chimie ParisTech. V.B. is grateful to the Swiss excellence scholarships for financial support, scholarship number 2017.0801.

References

1. Colley DG, Bustinduy AL, Secor WE, King CH. Human schistosomiasis. Lancet (London, England). 2014;383(9936):2253-64.
2. Rotger M, Serra T, de Cárdenas MG, Morey A, Vicente MA. Increasing incidence of imported schistosomiasis in Mallorca, Spain. European Journal of Clinical Microbiology and Infectious Diseases. 2004;23(11):855-6.
3. Berry A, Moné H, Iriart X, Mouahid G, Aboo O, Boissier J, et al. Schistosomiasis Haematobium, Corsica, France. Emerging Infectious Diseases. 2014;20(9):1595-7.
4. Steinmann P, Keiser J, Bos R, Tanner M, Utzinger J. Schistosomiasis and water resources development: systematic review, meta-analysis, and estimates of people at risk. The Lancet Infectious Diseases. 2006;6(7):411-25.
5. Bergquist R, Zhou X-N, Rollinson D, Reinhard-Rupp J, Klohe K. Elimination of schistosomiasis: the tools required. Infect Dis Poverty. 2017;6(1):158-.
6. Geerts S, Gryseels B. Drug Resistance in Human Helminths: Current Situation and Lessons from Livestock. Clinical Microbiology Reviews. 2000;13(2):207-22.
7. Lago EM, Xavier RP, Teixeira TR, Silva LM, da Silva Filho AA, de Moraes J. Antischistosomal agents: state of art and perspectives. Future Medicinal Chemistry. 2017;10(1):89-120.
8. Pica-Mattoccia L, Novi A, Cioli D. Enzymatic basis for the lack of oxamniquine activity in Schistosoma haematobium infections. Parasitology Research. 1997;83(7):687-9.
9. Sabah AA, Fletcher C, Webbe G, Doenhoff MJ. Schistosoma mansoni: Chemotherapy of infections of different ages. Experimental Parasitology. 1986;61(3):294-303.
10. Pica-Mattoccia L, Carlini D, Guidi A, Cimica V, Vigorosi F, Cioli D. The schistosome enzyme that activates oxamniquine has the characteristics of a sulfotransferase. Memórias do Instituto Oswaldo Cruz. 2006;101:307-12.
11. Valentim CLL, Cioli D, Chevalier FD, Cao X, Taylor AB, Holloway SP, et al. Genetic and molecular basis of drug resistance and species-specific drug action in Schistosome parasites. Science (New York, NY). 2013;342(6164):1385-9.
12. Chevalier FD, Le Clec'h W, Eng N, Rugel AR, Assis RRd, Oliveira G, et al. Independent origins of loss-of-function mutations conferring oxamniquine resistance in a Brazilian schistosome population. International Journal for Parasitology. 2016;46(7):417-24.
13. Rugel A, Tarpley RS, Lopez A, Menard T, Guzman MA, Taylor AB, et al. Design, Synthesis, and Characterization of Novel Small Molecules as Broad Range Antischistosomal Agents. ACS Med Chem Lett. 2018;9(10):967-+.
14. Hillard EA, Vessières A, Jaouen G. Ferrocene Functionalized Endocrine Modulators as Anticancer Agents. In: Jaouen G, Metzler-Nolte N, editors. Medicinal Organometallic Chemistry. Berlin, Heidelberg: Springer Berlin Heidelberg; 2010. p. 81-117.
15. Biot C, Dive D. Bioorganometallic Chemistry and Malaria. In: Jaouen G, Metzler-Nolte N, editors. Medicinal Organometallic Chemistry. Berlin, Heidelberg: Springer Berlin Heidelberg; 2010. p. 155-93.
16. Gasser G, Metzler-Nolte N. The potential of organometallic complexes in medicinal chemistry. Current Opinion in Chemical Biology. 2012;16(1):84-91.
17. Patra M, Gasser G. The medicinal chemistry of ferrocene and its derivatives. Nature Reviews Chemistry. 2017;1(9):0066.
18. Ong YC, Roy S, Andrews PC, Gasser G. Metal Compounds against Neglected Tropical Diseases. Chemical reviews. 2019;119(2):730-96.
19. Dubar F, Egan TJ, Pradines B, Kuter D, Ncokazi KK, Forge D, et al. The antimalarial ferroquine: role of the metal and intramolecular hydrogen bond in activity and resistance. ACS chemical biology. 2011;6(3):275-87.
20. Keiser J, Vargas M, Rubbiani R, Gasser G, Biot C. In vitro and in vivo antischistosomal activity of ferroquine derivatives. Parasit Vectors. 2014;7:424.

21. Biot C, Taramelli D, Forfar-Bares I, Maciejewski LA, Boyce M, Nowogrocki G, et al. Insights into the mechanism of action of ferroquine. Relationship between physicochemical properties and antiplasmodial activity. Mol Pharm. 2005;2(3):185-93.
22. Hess J, Panic G, Patra M, Mastrobuoni L, Spingler B, Roy S, et al. Ferrocenyl, Ruthenocenyl, and Benzyl Oxamniquine Derivatives with Cross-Species Activity against Schistosoma mansoni and Schistosoma haematobium. ACS infectious diseases. 2017;3(9):645-52.
23. Hess J, Keiser J, Gasser G. Toward organometallic antischistosomal drug candidates. Future Medicinal Chemistry. 2015;7(6):821-30.
24. Buchter V, Hess J, Gasser G, Keiser J. Assessment of tegumental damage to Schistosoma mansoni and S. haematobium after in vitro exposure to ferrocenyl, ruthenocenyl and benzyl derivatives of oxamniquine using scanning electron microscopy. Parasites & Vectors. 2018;11(1):580.
25. Lombardo FC, Pasche V, Panic G, Endriss Y, Keiser J. Life cycle maintenance and drug-sensitivity assays for early drug discovery in Schistosoma mansoni. Nature Protocols. 2019:1.
26. 5 Human Albumin. Transfusion Medicine and Hemotherapy. 2009;36(6):399-407.
27. Keiser J. In vitro and in vivo trematode models for chemotherapeutic studies. Parasitology. 2010;137(3):589-603.
28. Faust EC, Jones CA. Life History of Manson's Blood Fluke (Schistosoma mansoni). III. The Blood Picture in Schistosomiasis Mansoni. Proceedings of the Society for Experimental Biology and Medicine. 1934;31(4):478-9.
29. Taylor AB, Pica-Mattoccia L, Polcaro CM, Donati E, Cao X, Basso A, et al. Structural and Functional Characterization of the Enantiomers of the Antischistosomal Drug Oxamniquine. PLOS Neglected Tropical Diseases. 2015;9(10):e0004132.
30. Taylor AB, Roberts KM, Cao X, Clark NE, Holloway SP, Donati E, et al. Structural and enzymatic insights into species-specific resistance to schistosome parasite drug therapy. Journal of Biological Chemistry. 2017;292(27):11154-64.
31. Frisch MJ, Trucks GW, Schlegel HB, Scuseria GE, Robb MA, Cheeseman JR, et al. Gaussian 16 Rev. B.01. Wallingford, CT2016.
32. Bayly CI, Cieplak P, Cornell W, Kollman PA. A well-behaved electrostatic potential based method using charge restraints for deriving atomic charges: the RESP model. The Journal of Physical Chemistry. 1993;97(40):10269-80.
33. D.A. Case RMB, D.S. Cerutti, T.E. Cheatham, III, T.A. Darden, R.E. Duke, T.J. Giese, H. Gohlke, A.W. Goetz, N. Homeyer, S. Izadi, P. Janowski, J. Kaus, A. Kovalenko, T.S. Lee, S. LeGrand, P. Li, C. Lin, T. Luchko, R. Luo, B. Madej, D. Mermelstein, K.M. Merz, G. Monard, H. Nguyen, H.T. Nguyen, I. Omelyan, A. Onufriev, D.R. Roe, A. Roitberg, C. Sagui, C.L. Simmerling, W.M. Botello-Smith, J. Swails, R.C. Walker, J. Wang, R.M. Wolf, X. Wu, L. Xiao and P.A. Kollman AMBER 2016. University of California, San Francisco. 2016.
34. Doman TN, Landis CR, Bosnich B. Molecular mechanics force fields for linear metallocenes. Journal of the American Chemical Society. 1992;114(18):7264-72.
35. Fiser A, Do RK, Sali A. Modeling of loops in protein structures. Protein science : a publication of the Protein Society. 2000;9(9):1753-73.
36. Ryckaert J-P, Ciccotti G, Berendsen HJC. Numerical integration of the cartesian equations of motion of a system with constraints: molecular dynamics of n-alkanes. Journal of Computational Physics. 1977;23(3):327-41.
37. Miller BR, McGee TD, Swails JM, Homeyer N, Gohlke H, Roitberg AE. MMPBSA.py: An Efficient Program for End-State Free Energy Calculations. Journal of Chemical Theory and Computation. 2012;8(9):3314-21.
38. Patra M, Ingram K, Leonidova A, Pierroz V, Ferrari S, Robertson MN, et al. In Vitro Metabolic Profile and in Vivo Antischistosomal Activity Studies of (η6-Praziquantel)Cr(CO)3 Derivatives. Journal of Medicinal Chemistry. 2013;56(22):9192-8.
39. Keller S, Ong YC, Lin Y, Cariou K, Gasser G. A tutorial for the assessment of the stability of organometallic complexes in biological media. Journal of Organometallic Chemistry. 2020;906:121059.
40. Tan J, Sivaram H, Huynh HV. Gold(I) bis(N-heterocyclic carbene) complexes: Metabolic stability, in vitro inhibition, and genotoxicity. 2018;32(8):e4441.

41. Heurtault B, Saulnier P, Pech B, Proust J-E, Benoit J-P. A Novel Phase Inversion-Based Process for the Preparation of Lipid Nanocarriers. Pharmaceutical Research. 2002;19(6):875-80.
42. Pasche V, Laleu B, Keiser J. Screening a repurposing library, the Medicines for Malaria Venture Stasis Box, against Schistosoma mansoni. Parasites & Vectors. 2018;11:298.
43. Olliaro P, Delgado-Romero P, Keiser J. The little we know about the pharmacokinetics and pharmacodynamics of praziquantel (racemate and R-enantiomer). Journal of Antimicrobial Chemotherapy. 2014;69(4):863-70.
44. Keen P. Effect of Binding to Plasma Proteins on the Distribution, Activity and Elimination of Drugs. In: Brodie BB, Gillette JR, Ackerman HS, editors. Concepts in Biochemical Pharmacology: Part 1. Berlin, Heidelberg: Springer Berlin Heidelberg; 1971. p. 213-33.
45. Measurement of in vitro intrinsic clearance using microsomes [Available from: https://www.cyprotex.com/admepk/in-vitro-metabolism/microsomal-stability.
46. Colleen A. McNaney DMD, Serhiy Y. Hnatyshyn, Tatyana A. Zvyaga, Jay O. Knipe, James V. Belcastro, and Mark Sanders. An Automated Liquid Chromatography-Mass Spectrometry Process to Determine Metabolic Stability Half-Life and Intrinsic Clearance of Drug Candidates by Substrate Depletion. 2008;6(1):121-9.
47. Słoczyńska K, Gunia-Krzyżak A, Koczurkiewicz P, Wójcik-Pszczoła K, Żelaszczyk D, Popiół J, et al. Metabolic stability and its role in the discovery of new chemical entities. 2019;69(3):345.
48. Huynh NT, Passirani C, Saulnier P, Benoit JP. Lipid nanocapsules: a new platform for nanomedicine. Int J Pharm. 2009;379(2):201-9.
49. Laine AL, Huynh NT, Clavreul A, Balzeau J, Bejaud J, Vessieres A, et al. Brain tumour targeting strategies via coated ferrociphenol lipid nanocapsules. European journal of pharmaceutics and biopharmaceutics : official journal of Arbeitsgemeinschaft fur Pharmazeutische Verfahrenstechnik eV. 2012;81(3):690-3.
50. Allard E, Jarnet D, Vessieres A, Vinchon-Petit S, Jaouen G, Benoit JP, et al. Local delivery of ferrociphenol lipid nanocapsules followed by external radiotherapy as a synergistic treatment against intracranial 9L glioma xenograft. Pharm Res. 2010;27(1):56-64.
51. Karim R, Lepeltier E, Esnault L, Pigeon P, Lemaire L, Lepinoux-Chambaud C, et al. Enhanced and preferential internalization of lipid nanocapsules into human glioblastoma cells: effect of a surface-functionalizing NFL peptide. Nanoscale. 2018;10(28):13485-501.
52. Laine AL, Adriaenssens E, Vessieres A, Jaouen G, Corbet C, Desruelles E, et al. The in vivo performance of ferrocenyl tamoxifen lipid nanocapsules in xenografted triple negative breast cancer. Biomaterials. 2013;34(28):6949-56.

TOC Graphic (TIFF format)